Trans. Phenom. Nano Micro Scales, 2(1): 65-77, Winter - Spring 2014
DOI: 10.7508/tpnms.2014.01.006

ORIGINAL RESEARCH PAPER

Numerical Investigation of Double- Diffusive Mixed Convective Flow in a Lid-Driven Enclosure Filled with Al_2O_3-Water Nanofluid

A. Fattahi [1,*], M. Alizadeh[1]
[1] *Mechanical Engineering Department, Iran University of Science and Technology, Narmak, Tehran, I.R. Iran*

ARTICLE INFO:

Article history:
Received 3 Octobre 2013
Accepted 20 December 2013

Keywords:
Al2O3-water nanofluid
Double- diffusion
Mixed convection
Variable properties

Abstract

Double-diffusive mixed convection in a lid-driven square enclosure filled with Al_2O_3-water is numerically investigated. Two-dimensional nonlinear governing equations are discretized using the control volume method and hybrid scheme. The equations are solved using SIMPLER algorithm. The results are displayed in the form of streamlines, isotherms, and iso-concentrations when the Richardson number varies between 0.01 and 100, the Lewis number changes from 0.1 to 10, the buoyancy ratio ranges between 0 and 5,the volume fractions of nanoparticles differs from 0 to 0.06 and the source location moves from the top toward bottom of the left wall. Moreover, the variation of average Nusselt and Sherwood number are illustrated. It is observed that heat transfer enhances as nanoparticles volume fraction increases, while mass transfer reduces. Additionally, by increasing the buoyancy ratio, both heat and mass transfer are increased.

1. Introduction

Mixed convection of heat transfer has been a subject of interest in recent years due to its applications, especially those related to lubrication technology, electronic cooling, food processing and float glass manufacturing [1-2]. Double-diffusive convection is the simultaneous heat and mass transfer in which bouyancy-driven flow is induced by both temperature and concentration gradients [3-4]. The two buoyancy forces may act in aiding or opposing directions. Double diffusion occurs in many processes in industry and environment including the transport of water vapor and other chemical contaminants across confined spaces. Deng et al. [5] investigated laminar double-diffusive mixed convection in a two-dimensional ventilated enclosure. Their results presented in the form of streamlines, heatlines and masslines. They tried to minimize heat and mass transfer by proposing a correlation between Reynolds and Grashof numbers. Al-Amiri et al. [6] investigated steady mixed convection in a square lid-driven cavity under the combined buoyancy effects of thermal and mass diffusion. The transport equations were numerically solved using the Galerkin weighted residual method. The results demonstrated the range where high heat and mass transfer rates can be attained for a given Richardson number. Beya and Lili [7] studied the unsteady double-diffusive mixed convection in two-dimensional ventilated room. Their study is similar to work of Deng et al. [5] except unsteady conditions. Teamah and El-Maghlany [8] concerned with the mixed convection in a rectangular

[*]Corresponding author
Email Address: abolfazl.fattahi@yahoo.com

lid-driven cavity. Their numerical results were reported for the effect of Richardson number, Lewis number, and buoyancy ratio on the iso-contours of streamline, temperature, and concentration for Richardson number varied between 0.01 to 104 and the buoyancy ratio changes -10 to 10. They concluded that when buoyancy ratio values is negative, the heat transfer in assisting flow is less than that in opposing flow for high values of the Richardson number. A major limitation against enhancing heat transfer in convective heat transfer is inherently low thermal properties of working fluids, such as, air, water and ethylene glycol. Suspending different types of small solid particle in a base fluid is an innovative way to overcome this limitation. A dilute suspension of solid nanoparticles is called a nanofluid.

Nomenclature

c	Concentration
C	Dimensionless concentration
D	Mass diffusivity
H	Enclosure height
L	Thickness of enclosure
Le	Lewis number (Sc/Pr)
N	Buoyancy ratio
Nu	Nusselt number
p	Pressure
P	Dimensionless pressure
Pr	Prandtl number
Ra	Rayleigh number
Ri	Richardson number
Sh	Sherwood number
T	Temperature
u, v	Components of velocity
U, V	Dimensionless velocity components
U_p	Movable plate velocity
X, Y	Dimensionless Cartesian coordinates
x,y	Cartesian coordinates
Y_D	Source location

Greek symbols

α	Thermal diffusivity
θ	Dimensionless temperature
φ	Volume fraction
β	Volumetric coefficient

Subscript

avg	Average
c	Cold wal
h	Hot wall
T	Thermal
M	Mass
nf	Nanofluid
p	Particle

Talebi et al. [9] studied laminar mixed convection flows through a copper-water nanofluid in a square lid-driven cavity. Their study was carried out for the Rayleigh number 104 to 106, Reynolds number 1 to 100 and the solid volume fraction 0 to 0.05. The thermal conductivity and effective viscosity of nanofluid calculated by Patel and Brinkman models, respectively. It was observed that the effect of solid concentration decreases by increasing Reynolds number. Nemati et al. [10] surveyed mixed convection flows in a lid-driven cavity filled with Cu, CuO or Al_2O_3-water nanofluids utilizing Lattice Boltzmann Method. Their results indicated that the effects of solid volume fraction grow stronger sequentially for Al_2O_3, CuO and Cu nanoparticles. Chamkha and Abu-Nada [11] used two nanofluid viscosity model in the simulation of steady laminar mixed convection flow in single and double-lid square cavities filled with a Al_2O_3-water nanofluid. They found that significant heat transfer enhancement can be obtained due to the presence of nanoparticles and this is accentuated by increasing the nanoparticle volume fractions at moderate and large Richardson numbers for both single- and double-lid cavity configurations. In the other study, Abu-Nada et al. [12] investigated the role of nanofluid variable properties in differentially heated enclosures and found that nanofluid variable properties play a determinative role in the prediction of heat transfer enhancement.

In the present study, mixed convection in a lid-driven square enclosure filled with Al2O3-water nanofluid is numerically investigated. To the best our knowledge, no research has been done in the double-diffusion mixed convection with considering nanoparticles blended in a base fluid. The properties

of nanofluid are defined as the function of temperature and nanopartcles volume fraction. The effect of of pertinent parameters, such as, Richardson number, Lewis number, buoyancy ratio, nanoparticles volume fraction and the source location on the flow field, heat and mass transfer is studied.

2.Physical model and the problem formulation

….A schematic diagram of the enclosure with the same width and height, L, is shown in Fig. 1. A source with high temperature and concentration (Th, Ch) is placed along the left wall, while the right wall of the enclosure is kept at low temperature and concentration (Tc, Cc). The length of the source is equal to L/2 (Fig. 1). The horizontal top and the bottom walls of the enclosure, as well as, the inactive portion of the left wall are kept insulated and impermeable. The top wall of the enclosure moves to the right direction with a constant velocity, Up. The location of the source on the left wall is shown by h. The dimensionless variable, YD, for the location of the source is defined as YD= h/L.

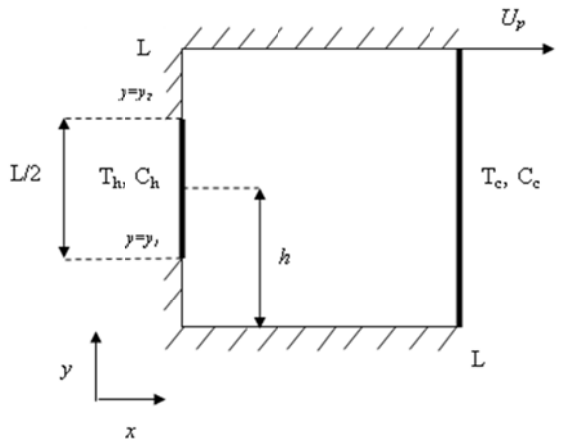


Fig.1. Physical model and the boundary conditions of the present study

The Boussinesq approximation holds, meaning that density is linearly proportional to both temperature and concentration.

$$\rho = \rho_0(1-\beta_T(T-T_c)-\beta_M(c-c_c)) \tag{1}$$

The enclosure is filled with the Al_2O_3-water nanofluid. The nanofluid in the enclosure is Newtonian, incompressible and viscous. The viscous dissipation is assumed to be negligible. The heat flux driven by concentration gradients (Soret effect) and the mass flux driven by temperature gradients (Dufour effect) are neglected. In addition, it is assumed that both the fluid phase and nanoparticles are in the thermal equilibrium state and they flow with the same velocity. The nanoparticles are assumed to have uniform shape and size. The thermal conductivity and the viscosity of the nanofluid are taken into consideration as variable properties; both of them change with volume fraction and temperature of nanoparticles. Under the above assumptions, the system of governing equations is:

Continuity equation

$$\frac{\partial u}{\partial x}+\frac{\partial v}{\partial y}=0 \tag{2}$$

x-momentum equation:

$$\rho_{nf}(u\frac{\partial v}{\partial x}+v\frac{\partial v}{\partial y}) = -\frac{\partial p}{\partial y}+\frac{\partial}{\partial x}\left(\mu_{nf}\frac{\partial v}{\partial x}\right)+\frac{\partial}{\partial y}\left(\mu_{nf}\frac{\partial v}{\partial y}\right)+[\varphi\rho_p\beta_T+(1-\varphi)\rho_f\beta_T]g(T-T_c)+\varphi\rho_p\beta_M+(1-\varphi)\rho_f\beta_M]g(c-c_c) \tag{3}$$

y-momentum equation:

$$\rho_{nf}\left(u\frac{\partial V}{\partial x}+v\frac{\partial V}{\partial y}\right) = -\frac{\partial P}{\partial y}+\frac{\partial}{\partial x}\left(\mu_{nf}\frac{\partial V}{\partial x}\right)+\frac{\partial}{\partial y}\left(\mu_{nf}\frac{\partial V}{\partial y}\right)+[\varphi\rho_p\beta_T+(1-\varphi)\rho_f\beta_T]g(T-T_c)+[\varphi\rho_p\beta_M+(1-\varphi)\rho_f\beta_{Mf}]g(C-C_c) \tag{4}$$

Energy equation:

$$(\rho c_p)_{nf}\left(u\frac{\partial T}{\partial x}+v\frac{\partial T}{\partial y}\right) = \frac{\partial}{\partial x}\left(k_{nf}\frac{\partial T}{\partial x}\right)+\frac{\partial}{\partial y}\left(k_{nf}\frac{\partial T}{\partial y}\right) \tag{5}$$

Concentration equation:

$$u\frac{\partial c}{\partial x}+v\frac{\partial c}{\partial y}=\frac{\partial}{\partial x}(D\frac{\partial c}{\partial x})+\frac{\partial}{\partial y}(D\frac{\partial c}{\partial y}) \tag{6}$$

The effective density of the nanofluid at reference temperature is:

$$\rho_{nf} = (1-\varphi)\rho_f + \varphi\rho_{p,0} \tag{7}$$

and the specific heat capacity of nanofluid is

$$(\rho\beta)_{nf} = (1-\varphi)(\rho\beta)_f + \varphi(\rho\beta)_p \tag{8}$$

$$(\rho c_p)_{nf} = (1-\varphi)(\rho c_p)_f + \varphi(\rho c_p)_p \tag{9}$$

The effective thermal conductivity of the nanofluid calculated by the Chon et al. [13, 14] model is:

$$\frac{k_{nf}}{k_f} = 1 + 64.7\varphi^{0.4076}\left(\frac{d_f}{d_p}\right)^{0.3690} \left(\frac{k_p}{k_f}\right)^{0.7476} pr_T^{0.9955} Re^{1.2321} \tag{10}$$

where pr_T and Re are defined by:

$$Pr_T = \frac{\mu_f}{\rho_f \alpha_f} \tag{11}$$

$$Re = \frac{\rho_f k_b T}{3\pi\mu_f l_f} \tag{12}$$

kb=1.3807×10^{-23} J/K, is the Boltzmann constant and lf=0.17 nm is the mean path of fluid particles [13, 14]. The viscosity of the nanoparticle (Al_2O_3) as given by Nguyen et al. [14, 15] is:

$$\mu_{nf} = \exp(3.003 - 0.04203T - 0.5445\varphi + 0.0002553T^2 + 0.524\varphi^2 - 1.622\varphi^{-1}) \times 10^{-3} \tag{13}$$

The viscosity of the base fluid (water) is considered as a function of temperature. The following equation is used to obtain the viscosity of water [14, 15]:

$$\mu_f = (1.2723ln^5T - 8.736ln^4T + 33.708ln^3T - 246.6ln^2T + 518.78lnT + 1153.9) \times 10^{-6} \tag{14}$$

Using the following dimensionless variables, the equations are written in dimensionless form.

$$X = \frac{x}{L}, \quad Y = \frac{y}{L}, \quad U = \frac{u}{U_p}, \quad V = \frac{v}{U_p}, \quad P = \frac{p}{\rho_{nf}U_P^2}, \quad \theta = \frac{T-T_c}{T_h-T_c}, \quad C = \frac{c-c_c}{c_h-c_c}, \tag{15}$$

The dimensionless form of the governing equations becomes as follows:

Continuity equation:

$$\frac{\partial U}{\partial X} + \frac{\partial V}{\partial Y} = 0 \tag{16}$$

x-momentum equation:

$$U\frac{\partial U}{\partial X} + V\frac{\partial U}{\partial Y} = -\frac{\partial P}{\partial X} + \frac{\partial}{\partial X}\left(\frac{1}{Re^*}\frac{\partial U}{\partial X}\right) + \frac{\partial}{\partial Y}\left(\frac{1}{Re^*}\frac{\partial U}{\partial Y}\right) \tag{17}$$

y-momentum equation:

$$U\frac{\partial V}{\partial X} + V\frac{\partial V}{\partial Y} = \frac{\partial P}{\partial Y} + \frac{\partial}{\partial X}\left(\frac{1}{Re^*}\frac{\partial V}{\partial X}\right) + \frac{\partial}{\partial Y}\left(\frac{1}{Re^*}\frac{\partial V}{\partial Y}\right) + Ri^*(\theta + NC) \tag{18}$$

Energy equation:

$$U\frac{\partial \theta}{\partial X} + V\frac{\partial \theta}{\partial Y} = \frac{1}{\alpha_f \times (\rho c_p)_{nf}}\left[\frac{\partial}{\partial X}\left(\frac{K_{nf}}{Re^*Pr^*}\frac{\partial \theta}{\partial X}\right) + \frac{\partial}{\partial Y}\left(\frac{k_{nf}}{Re^*Pr^*}\frac{\partial \theta}{\partial Y}\right)\right] \tag{19}$$

Concentration equation:

$$U\frac{\partial C}{\partial X} + V\frac{\partial C}{\partial Y} = \frac{\partial}{\partial X}\left(\frac{1}{Le^*Re^*Pr^*}\frac{\partial C}{\partial X}\right) + \frac{\partial}{\partial Y}\left(\frac{1}{Le^*Re^*Pr^*}\frac{\partial C}{\partial Y}\right) \tag{20}$$

Where

$$Pr^* = \frac{\mu_{nf}}{\mu_f}\frac{C_{P_{nf}}}{C_{P_f}}\frac{k_f}{k_{nf}}Pr, \qquad Le^* = \frac{\rho_f}{\rho_{nf}}\frac{C_{P_f}}{C_{P_{nf}}}\frac{k_{nf}}{k_f}Le,$$

$$Re^* = \frac{\rho_{nf}}{\rho_f}\frac{\mu_f}{\mu_{nf}}Re, \qquad Ri^* = \frac{(\rho\beta)_{nf}}{\rho_{nf}\beta_f}Ri$$

Dimensionless boundary conditions are as follows:

$$\begin{aligned}
&X = 0, 0 \le Y \le 1 : U = V = 0,\\
&\theta = C = 1\\
&\partial\theta/\partial n = \partial C/\partial n = 0\\
&X = 1, 0 \le Y \le 1 :\\
&U = V = 0, \theta = C = 0\\
&Y = 0, 0 \le X \le 1 :\\
&U = V = 0, \partial\theta/\partial n = \partial C/\partial n = 0\\
&Y = 1, 0 \le X \le 1 :\\
&U = 1, V = 0, \partial\theta/\partial n = \partial C/\partial n = 0
\end{aligned} \tag{21}$$

where $\frac{\partial}{\partial n}$ denotes the derivative with respect to the normal direction. The average Nusselt and Sherwood numbers are calculated from the following relations:

$$Nu_{avg} = -2\frac{k_{nf}}{k_f}\int_{Y_1}^{Y_2}\left.\frac{\partial\theta}{\partial X}\right|_{X=0} dY \tag{22}$$

$$Sh_{avg} = -2\int_{Y_1}^{Y_2}\left.\frac{\partial C}{\partial X}\right|_{X=0} dY \tag{23}$$

where $Y_1 = y_1/L$ and $Y_2 = y_2/L$. The coordinates y_1 and y_2 are defined in Fig. 1.

3.Numerical method

The governing non-linear equations with the appropriate boundary conditions were solved by iterative numerical method using the finite volume technique. In order to couple the velocity and pressure field in the momentum equations, the well-known SIMPLER (semi-implicit method for pressure-linked equations revised) algorithm was adopted. Uniform grid is used for this problem. The set of linear algebraic equations was solved using TDMA (Three Diagonal Matrix Algorithm). The under-relaxation factors for *U*-velocity, *V*-velocity, energy, and concentration equations were 0.6, 0.6, 0.4, and 0.4, respectively.

4. Benchmarking of the code

To reach the grid independent solution, various grids (51×51, 91×91, 131×131, 171×171, 211×211 251×251and 291×291) were tested. Finally, it is found that the grid size of 251×251 is adequately appropriate to ensure a grid independent solution.

Fig. 2 and Fig. 3 present a comparison between the present work and the results of Teamah and El-Maghlany [8] and Esfahani and Bordbar [16], respectively. It is obvious that the two sets of results are in good agreement. It should be noted that this code was previously validated for several test problems [14]. Based on this successful validation, the code can be used to simulate the present problem.

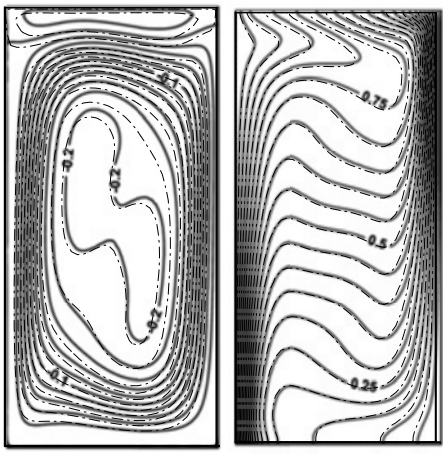


Fig. 2. Isotherm (right), Stream line (left) for *Le*=1, *N*=10, *Ri*=1 and U_{up}= -1,Ref. [8](solid lines), present work(dash lines)

5.Results and discussion

The effect of the bouyancy ratio, Lewis number,Richardson number and the source location on the double-diffusive mixed convection in the lid-driven square enclosure is numerically studied. For this sake, the countours of isotherms, streamlines and iso-concentrations, as well as, average values of Nusselt and Sherwood number are presented. The upper plate of the enclosure is moving toward right reusulting to an assisting flow. It means the forced convection helps to the natural convection from the hot left source to the cold right wall. The bouyancy

ratio varies between 0 to 5, Lewis number changes between 0.1 to 10, Richardson number ranges between 0.01 to 100,nanoparticles volume fraction differs from 0 to 0.06 and the source location moves from the top toward bottom of the left wall. All the results presented below are for the Prandtl number of the base fluid equal to 5.83.

5.1. Effect of the bouyancy ratio

Fig. 4 shows the effect of N on isotherms, streamlines and iso-concentrations for Ri=1, Le=1, Y_D=0.5 and various nanoparticles volume fractions.

As this figure shows, when $\varphi = 0.0$ and Le=1, the isotherms and iso-concentrations are similar to each other due to the similarity between the energy and concentration equations. Moreover, when N>0, the solutal and thermal buoyancy forces act in a same direction. At N = 0 and 0.2, the circulating cells are formed from the moving plate. Thermal and solutal boundary layers are also formed on the left source and top of the right wall. It demonstrates that increasing N remains no considerable effect on the heat and mass transfer occurs for N=5 compared to the other cases. In the whole N cases, streamlines have a unicellular shape.

Fig. 5 illustrates the variation of Nu_{avg} and Sh_{avg} versus nanoparticles volume fraction in various buoyancy ratios and Ri=1, Le=1 and Y_D=0.5. As Fig. 5 shows, the values of Nu_{avg} and Sh_{avg} at N=0 and 0.2 has no dramatic difference. By increasing N, both heat and mass transfer are increased. Nu_{avg} rises by increasing nanoparticles volume fraction. It is because of increasing conductive properties of the fluid by adding more nanoparticles. Unlike Nu_{avg} behavior, Sh_{avg} decreases as nanoparticles are added. It is due to increasing concentration by adding nanoparticles and consequently, decreasing the concentration gradient.

5.2.Effect of Lewis number

Le reflects a measure of thermal diffusivity of the fluid to its mass diffusivity. Le varies between 0.1 to 10 in the ongoing study. Fig. 6 shows the effect of Le on the isotherms, streamlins and iso-concentrations for Ri=1, N=1, Y_D=0.5 and various nanoparticles volume fractions. Variation of Le do not have any considerable effect on streamlines. Streamlines form in a unicellular structure as the resultant of both forced and natural convection. At Le=0.1, the core cell of nanofluid becomes smaller than that of the base fluid. On the other hand, variation of Le changes thickness of the boundary layers on the source and top of the right wall. By increasing Le, solutal boundary layer becomes denser, while thermal one turns into a thicker layer.

It should be noted that the change of Le does not have any drastic effect on isotherms. On the other the iso-concentrations vary severely by mitigating Le. According to the equations (19) and (20), one finds that the mass transfer is governed by Le, Re and Pr numbers, but heat transfer is governed by Re and Pr. When Pr, Re and φ are constant (as in Fig. 6), temperature doesn't have a dramatic change as the governing parameters in energy equation are fixed. On the other hand, mass transfer has a huge change by varying Le, because Le is a governing parameter in mass transfer equation. Thus, variation of Le can mainly affect mass transfer when other parameters are constant.

Fig. 7 represents the variation of Nu_{avg} and Sh_{avg} versus nanoparticles volume fraction in various Le and for Ri=1, N=1 and Y_D=0.5. As this figure shows, at low Le, Sh_{avg} cannot be assumed as a strong function of nanoparticles volume fraction. There is a very slight decrease in Sh_{avg} by increasing volume fraction at Le=0.1. At Le=10, mass transfer is decreased by adding more nanoparticles. Mass transfer increases as Le enhances as the result of densing solutal boundary layer. When Le increases, mass diffusion reduces and according to the continuity equation, mass is more transferred by bulk flow of the forced convection. Because of the stronger effect of bulk flow on mass transfer in comparison with the molecular diffusion, Sh_{avg} incraeses [17]. On the other hand, Nu_{avg} reduces when Le increases. As Le increases, thermal diffusivity increases ($\alpha = \frac{k}{\rho c_p}$). It causes conduction heat transfer to be stronger at high Le compared to the low Le cases where convection is stronger and dominant. Because conduction has a minor effect on heat transfer in comparison withconvection , Nu_{avg} reduces as Le increases. Similar to the previous case, Nu_{avg} increases by increasing nanoparticles volume fraction.

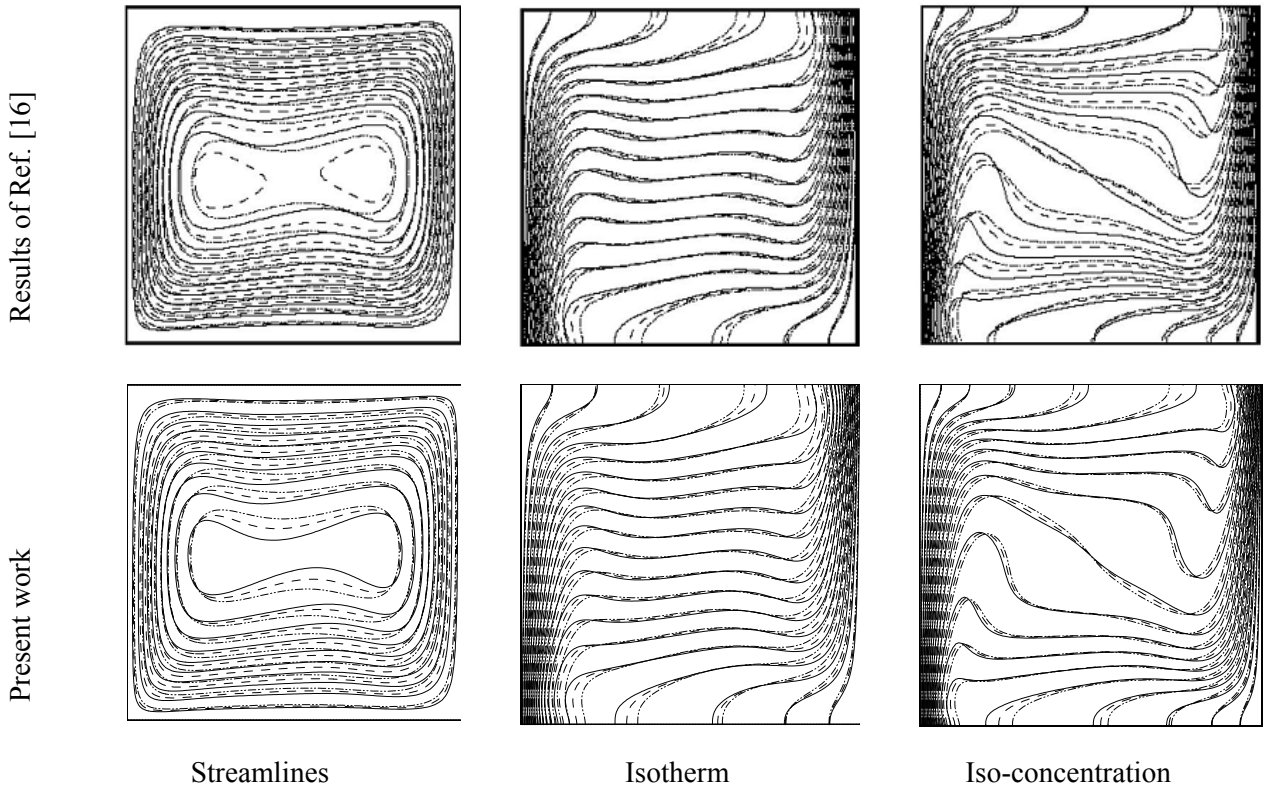


Fig. 3. Streamlines,isotherms and iso-concentrations for $\varphi = 0.0$(solid lines), $\varphi = 0.05$(dashed lines) and $\varphi = 0.1$ (dashe-dot-dot lines) at Ra=10^5 and Le=2: the comparison between the present work and the results of Ref. [16]

5.3.Effect of Richardson number

R_i provides the importance of natural canvection in comparison to the forced convection. The value of R_i varies from 0.01 to 100. Fig. 8 represents the effect of R_i on the isotherms, streamlines and iso-concentrations for various nanoparticles volume fractions when Le=1, N=1 and Y_D=0.5. At R_i=0.01, the forced convection is stronger than the natural one. Thus, the cells are fromed from the moving plate with a unicellular structure. The thin solutal and thermal boundary layers demonstrates a high heat and mass transfer. By incraesing R_i, the natural convection becomes stronger. Heat and mass transfer reduces as the boundary layers turn into a thicker ones. At R_i=100, the conduction is the governing heat transfer mechanism in the central zone of the enclosure. Furthermore, the flow core cell becomes wide except for$\varphi = 0.06$.

Fig. 9 shows the variation of Nu_{avg} and Sh_{avg} versus nanoparticles volume fractions in various Ri and for Le=1, N=1 and Y_D=0.5. As it is inferred form the boundary layers thichness, heat and mass transfer decreases when Ri increases.

5.4 Effect of the source location

Fig. 10 illustrates the effect of Y_D on the isotherms, streamlines and iso-concentrations for various nanoparticles volume fractions at Le=1, N=1 and Ri=1. By moving the source toward the bottom (decreasing Y_D), the recirculating cells extend to a larger zone of the enclosure. Fig. 11 shows the variation of Nu_{avg} and Sh_{avg} versus nanoparticles volume fractions in the various source locations and for Le=1, N=1 and Ri=1. As it is obvious heat and mass transfer enhances when the source moves toward the bottom of the left wall (decreasing Y_D).

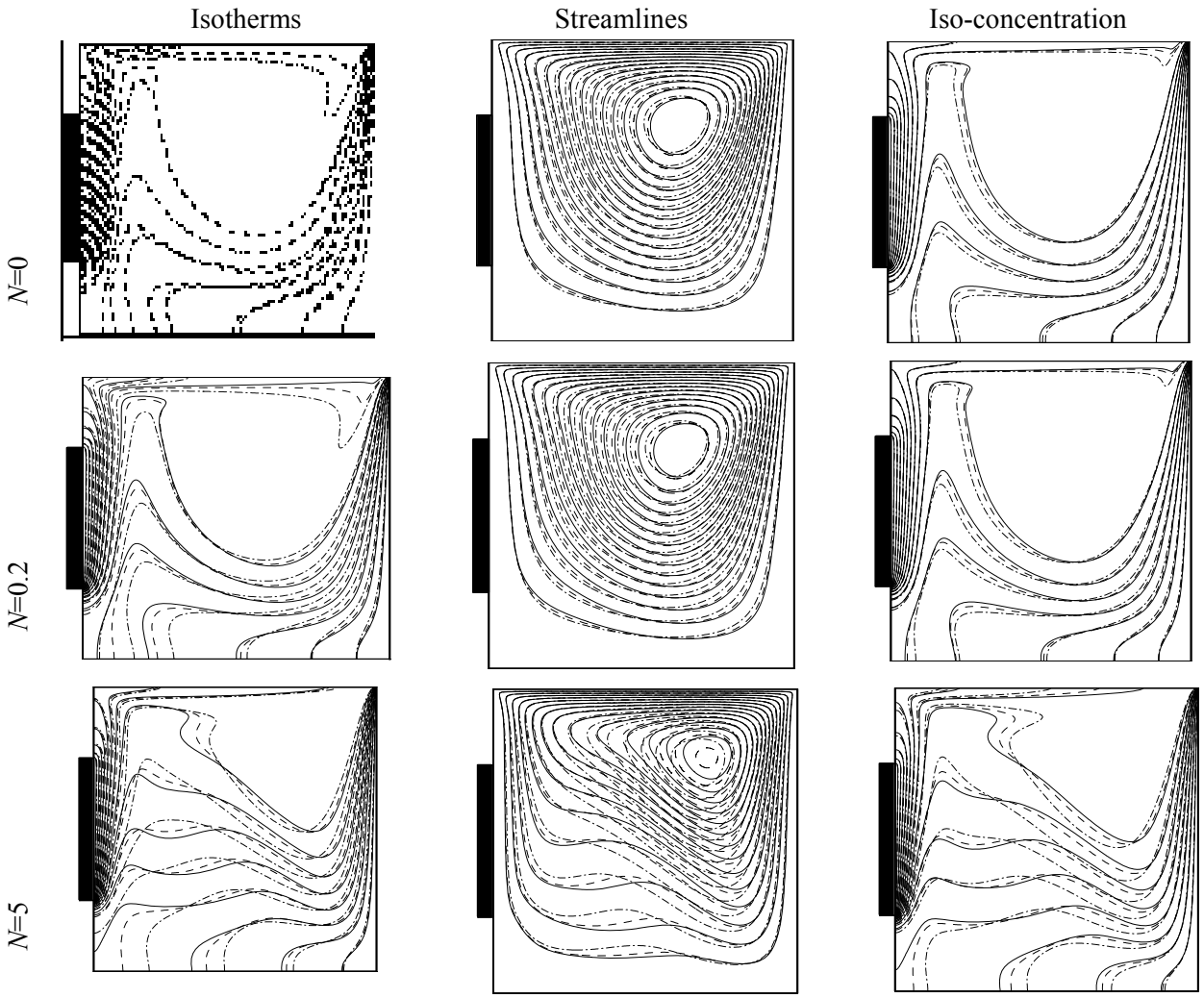


Fig. 4. Effect of buoyancy ratio (N) on the isotherms, streamlines and iso-concentrations for various nanoparticles volume fractions:
$\varphi = 0.0$ solid lines, $\varphi = 0.03$dash lines, $\varphi = 0.06$ dash-dot-dot lines (Ri=1, Le=1 and Y_D=0.5)

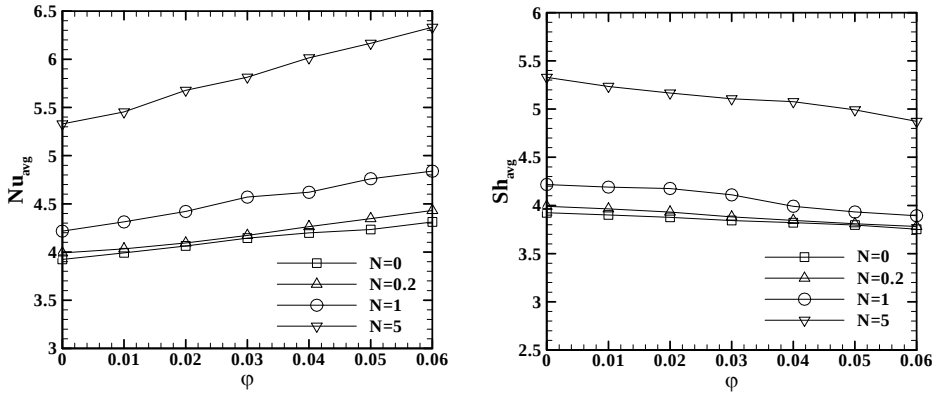


Fig. 5. Variation of average Nusselt and Sherwood number versus nanoparticles volume fraction in various bouyancy ratios (Ri=1, Le=1 and Y_D=0.5)

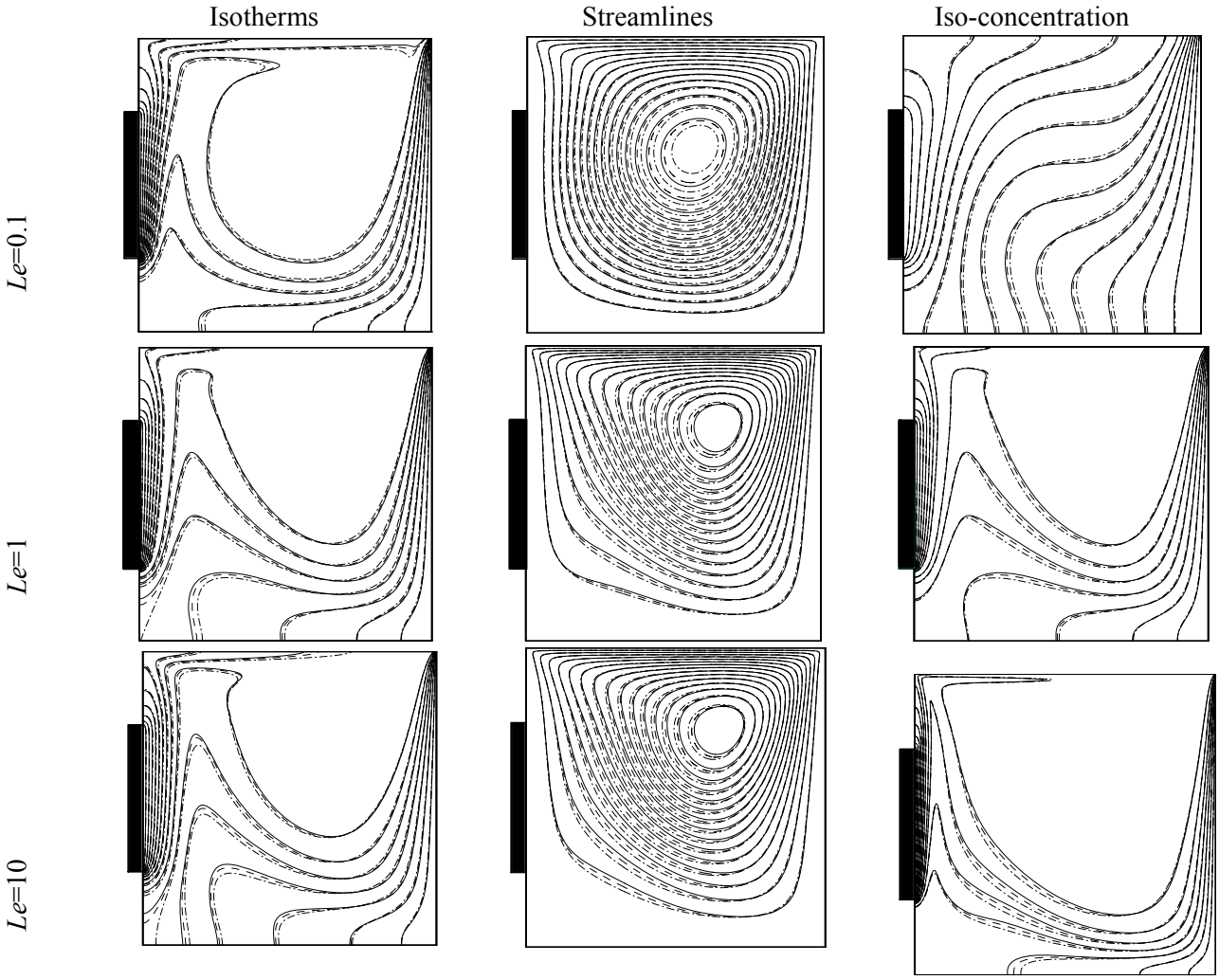


Fig. 6. Effect of Lewis number on the isotherms, streamlines and iso-concentrations for various nanoparticles volume fractions: $\varphi = 0.0$ solid lines, $\varphi = 0.03$dash lines, $\varphi = 0.06$dash-dot-dot lines (Ri=1, N=1 and Y_D=0.5)

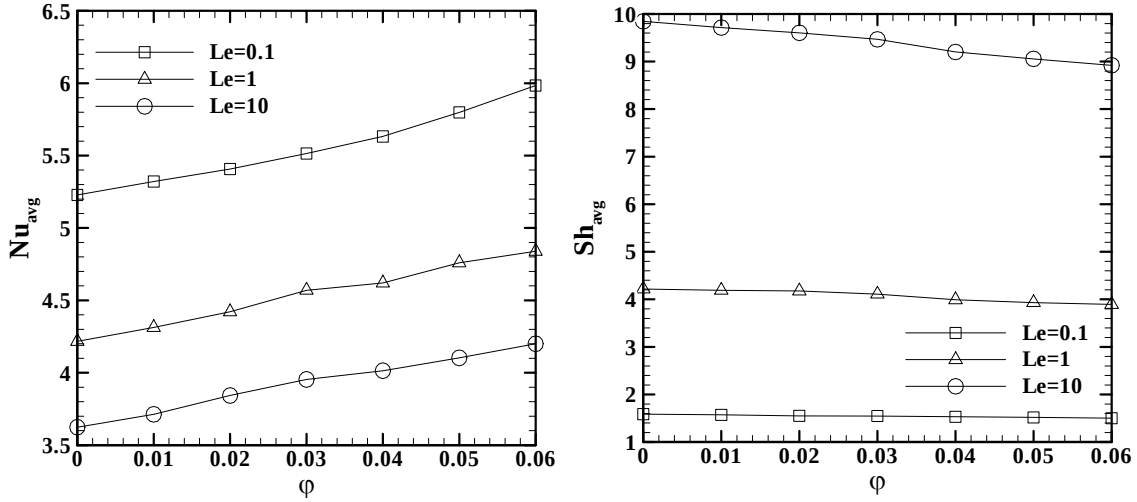


Fig. 7. : Variation of average Nusselt and Sherwood number versus nanoparticles volume fraction in various Lewis numbers (Ri=1, N=1 and Y_D=0.5)

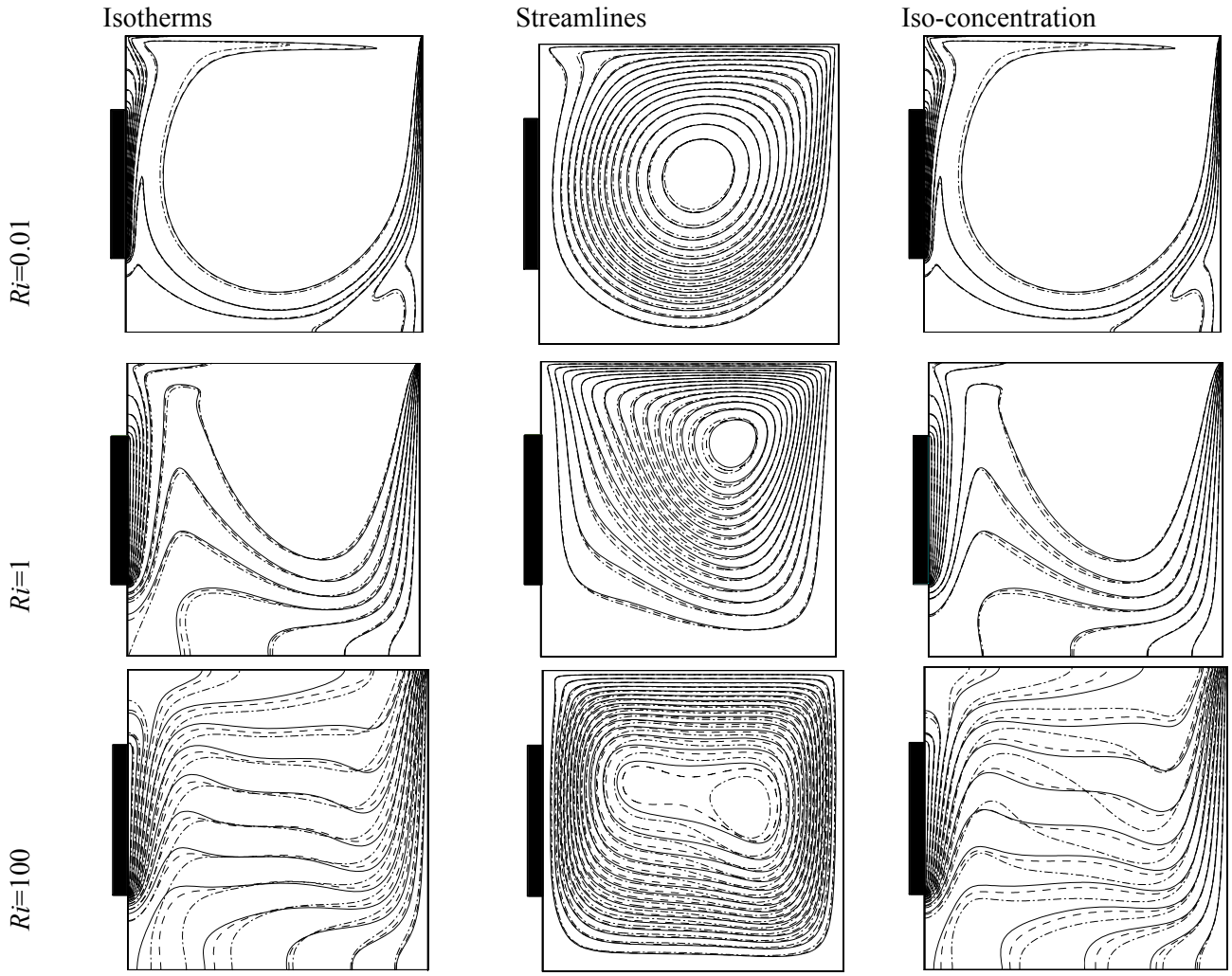


Fig. 8. Effect of Richardson number on the isotherms, streamlines and iso-concentrations for various nanoparticles volume fractions: $\varphi = 0.0$ solid lines, $\varphi = 0.03$dash lines, $\varphi = 0.06$dash-dot-dot lines (Le=1, N=1 and Y_D=0.5)

6. Conclusion

In this article, double-diffusive mixed convection in an enclosure filled with Al_2O_3-water nanofluid with a moving top plate is numerically studied. Based on the present study, the following results are obtained:

- By increasing the buoyancy ratio, both heat and mass transfer are increased.
- Average Nusselt number enhances as nanoparticles volume fraction increases, while average Sherwood number reduces
- Although average Sherwood number increases when Lewis number rises, average Nusselt number reduces.
- Heat and mass transfer decreases as Richardson number increases.
- Maximum heat and mass transfer occur when the source is located at the bottom of the left wall.

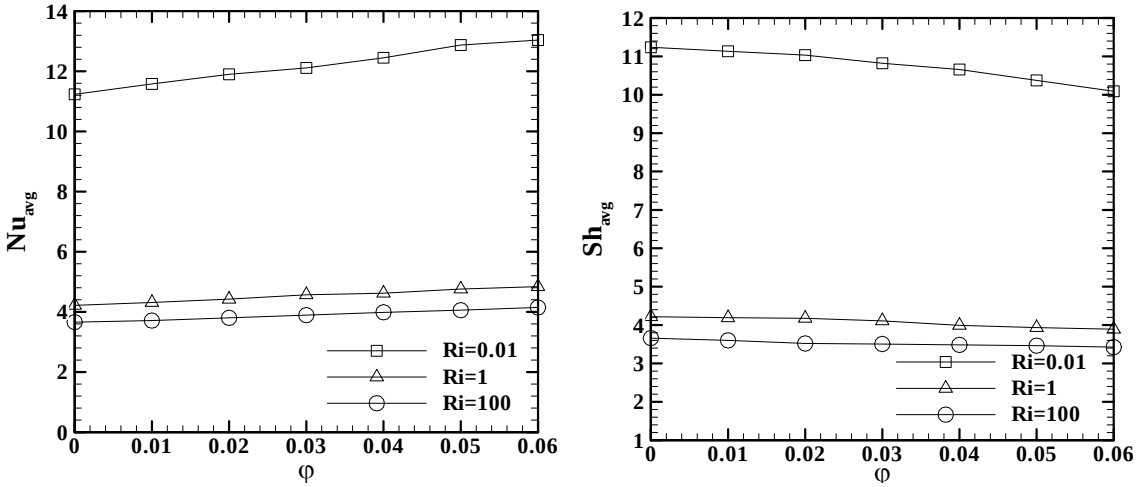


Fig. 9. : Variation of average Nusselt and Sherwood number versus nanoparticles volume fractions in various Richardson numbers (*Le*=1, *N*=1 and Y_D=0.5)

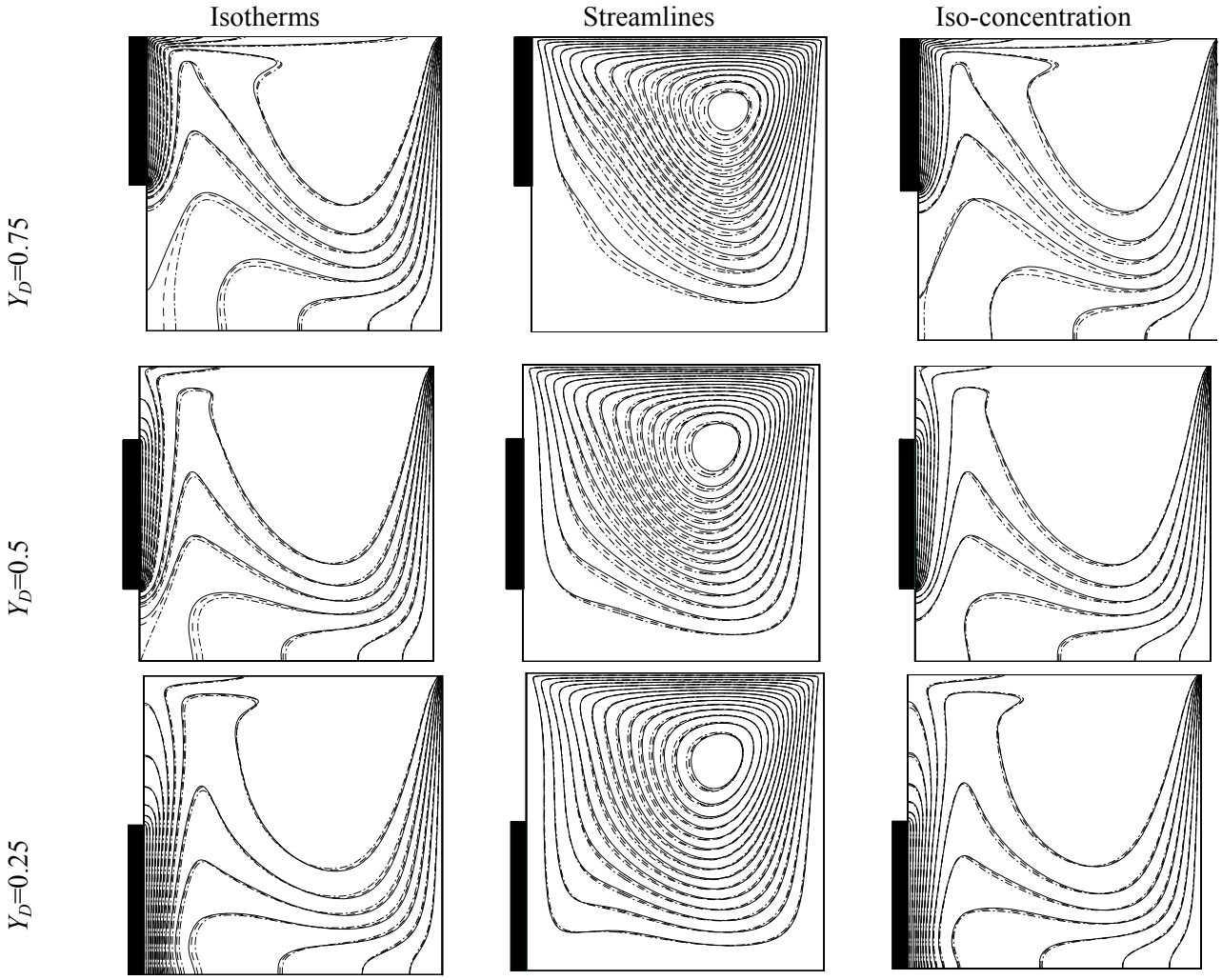


Fig. 10. Effect of the source location (Y_D) on the isotherms, streamlines and iso-concentrations for various nanoparticles volume fractions:
$\varphi = 0.0$ solid lines, $\varphi = 0.03$dash lines, $\varphi = 0.06$dash-dot-dot lines (*Le*=1, *N*=1 and *Ri*=1)

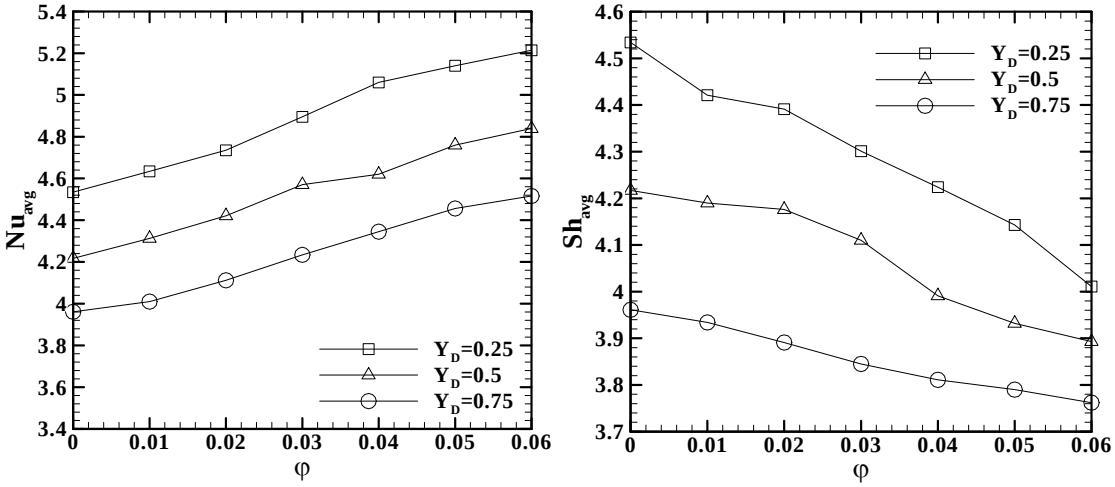


Fig. 11. Variation of average Nusselt and Sherwood number versus nanoparticles volume fractions in the various source location (*Le*=1, *N*=1 and *Ri*=1)

References

[1] B. Gebhart, L. Pera**:** The nature of vertical natural convection flows resulting from the combined buoyancy effects of thermal and mass diffusion, Int. J. Heat and Mass Transfer. 14 (1971) 2025-2050.

[2] A. Bejan**:** Mass and heat transfer by natural convection in a cavity, Int. J. Heat Fluid Flow. 6(3) (1985) 2125-2150.

[3] C. Beghein, F. Haghighat, F. Allard: Numerical study of double-diffusive natural convection in a square cavity, Int. J. Heat Mass Transf. 35 (1992) 833-846.

[4] A.J. Chamkha, H. Al-Naser: Hydro magnetic double-diffusive convection in a rectangular enclosure with opposing temperature and concentration gradients, Int. J. Heat Mass Transf. 45 (2002) 2465-2483.

[5] Q.H. Deng, J. Zhou, C.Mei, Y.M. Shen: Fluid, heat and contaminant transport structures of laminar double-diffusive mixed convection in a two-dimensional ventilated enclosure, Int. J. Heat Mass Transf. 47(24) (2004) 5257-5269.

[6] A. M. Al-Amiri, Kh. M. Khanafer, I. Pop: Numerical simulation of combined thermal and mass transport in a square lid-driven cavity, Int. J. Therm. Sci. 46(7) (2007) 662-671.

[7] B. B. Beya, T. Lili: Oscillatory double-diffusive mixed convection in a two-dimensional ventilated enclosure, Int. J. Heat Mass Transf. 50(23-24) (2007) 4540-4553.

[8] M. A. Teamah, W. M. El-Maghlany: Numerical simulation of double-diffusive mixed convective flow in rectangular enclosure with insulated moving lid, Int. J. Therm. Sci. 49(9) (2010) 1625-1638.

[9] F. Talebi, A. H. Mahmoudi, M. Shahi: Numerical study of mixed convection flows in a square lid-driven cavity utilizing nanofluid, Int. Commun. Heat Mass Transf. 37(1) (2010) 79-90.

[10] H. Nemati, M. Farhadi, K. Sedighi, E. Fattahi, A.A.R. Darzi: Lattice Boltzmann simulation of nanofluid in lid-driven cavity, Int. Commun. Heat Mass Transf. 37(10) (2010) 1528-1534.

[11] A. J. Chamkha, E. Abu-Nada: Mixed convection flow in single- and double-lid driven square cavities filled with water-Al_2O_3 nanofluid: Effect of viscosity models, Europ. J. Mech. B/Fluids. Available online 19 March 2012.

[12] E. Abu-Nada, Z. Masoud, H. Oztop, A. Campo: Effect of nanofluid variable properties on natural convection in enclosures, Int. J. Thermal Sci. 49 (2010) 479-491.

[13] C.H. Chon, K.D. Kihm, S.P. Lee, S.U.S. Choi: Empirical correlation finding the role of temperature and particle size for nanofluid

(Al_2O_3) thermal conductivity enhancement. Appl. Phys. Lett. 87 (2005) 153107.

[14] G.A. Sheikhzadeh, M. Ebrahim Qomi, N. Hajialigol and A. Fattahi: Numerical study of mixed convection flows in a lid-driven enclosure filled with nanofluid using variable properties. Results Phys. 2 (2012) 5-13.

[15] C.T. Nguyen, F. Desgranges, G. Roy, N. Galanis, T. Mare, S. Boucher, H. Angue Minsta: Temperature and particle-size dependent viscosity data for water-based nanofluids-hysteresis phenomenon. Int. J. Heat Fluid Flow. 28 (2007) 1492-1506.

[16] J. Abolfazli Esfahani, V. Bordbar: Double Diffusive Natural Convection Heat Transfer Enhancement in a Square Enclosure Using Nanofluids, J. Nanotech. Eng. Med. 2 (2011) 1-9.

[17] L. C. Thomas: Heat transfer: Mass transfer supplement, Printice-Hall, Englewood (1991).